

A New Iterative Method to Compute the Higher Order Contributions to the Scattered Field by Complex Structures

F. Saez de Adana, O. Gutiérrez, L. Lozano, M.F. Cátedra
 Dprt. de Ciencias de la Computación.
 Universidad de Alcalá ,28806 Alcalá de Henares (MADRID), SPAIN
 Fax: + 34 91 885 66 99
 email: kiko.saez@uah.es

Abstract – A method to compute the higher order contributions to the scattered field by complex structures is presented in this paper. The method is based on a new interpolation technique to represent the induced current with a very low amount of sample points and computational cost. The amplitude and phase of the current are represented separately. Both are defined by an interpolating function, which is built using Bézier surfaces. These functions provide the amplitude and the phase at any given point of the scattering surface in an easy way. The higher order contributions to the scattered field are obtained by using a new iterative method based on Physical Optics (PO) and the Stationary Phase Method (SPM) to compute the integral. The proposed method takes advantage of the saving in computation cost offered by the new representation of the currents reducing the order of the function which is necessary to minimize, in order to obtain the stationary phase points required to evaluate the PO integral. The results obtained show that the method is both efficient and accurate.

I. INTRODUCTION

The main contributions to the scattered field by a simple object in presence of an electromagnetic wave are mainly due to the first order effects (reflections or diffractions). However, if the complexity of the body increases (for example, an airplane, a satellite or a ship), then higher order contributions (double-reflections, diffraction-reflections, etc) become relevant, especially for certain angular margins. There are many other situations where higher order effects are relevant: the analysis of antennas onboard complex structures, the study of propagation in tunnels, the computation of the RCS of cavities, etc. In these cases, multiple reflections and /or diffractions generally, make the greatest contribution to the scattered field.

Traditionally, there are some approximate methods to tackle the problem of high order interactions for asymptotically high frequencies. The Image Method (IM) [1-3] obtains multiple reflections by repeatedly applying the Image Theory [4], calculating multiple images of the electromagnetic

source and from these the scattered field at the observation point. The main problem with this technique is that the reflecting surfaces must be flat. Another method is the Shooting and Bouncing Rays (SBR) approach, [5-8], in which tubes of rays are shot from the source in all directions. When the tube reaches the observation point after reflecting in the body surface, the previously computed field intensity level at that point is amended with the tube's contribution to the field level. The main problem with this method is the high number of rays that must be shot to obtain the scattered field accurately enough, making the computational cost very high. As it is stated in [9] an exceedingly large number of rays must be traced for very high frequencies (sometimes up to 350 points per square wavelength). Another important problem is the treatment of the diffraction due to the high number of tubes of rays in the Keller's cone produced when an incident tube of rays reaches an edge.

Other possibilities are the inverse methods based on the Geometrical Theory of Diffraction (GTD/UTD) [10,11] or the SPM [12], in which, given the structure, the source and the observation points, all the possible reflection and diffraction paths connecting the source with the observation points are obtained, taking into consideration the contribution of certain flash-points to the scattered field: reflection points in GTD/UTD or stationary phase points in SPM. The main problem with these methods is obtaining the flash-points on the surfaces involved.

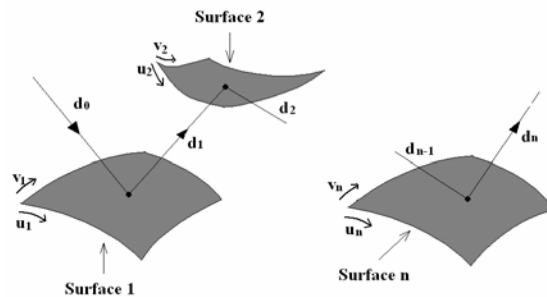


Fig. 1. Path to minimize for n reflections.

For example, Figure 1 shows a situation where a source and an observation point are placed in the vicinity of n arbitrary surfaces. If one wants to compute the reflected field at the observation point due to an n -order reflection in the surfaces of the scene, the first thing to do, using inverse methods, is to obtain the position of the n reflection points. If the geometrical surfaces are represented by parametrical surfaces (NURBS or Bézier surfaces [13,14]) as it is stated in [10] and [12], the reflection points are obtained after the minimization of the following function:

$$\begin{aligned}
 d^n(u_1, v_1, u_2, v_2, \dots, u_{n-1}, v_{n-1}, u_n, v_n) = & \\
 = d_0(u_1, v_1) + d_1(u_1, v_1, u_2, v_2) + & \\
 + d_2(u_2, v_2, u_3, v_3) + \dots + & \\
 + d_{n-1}(u_{n-1}, v_{n-1}, u_n, v_n) + d_n(u_n, v_n) & \quad (1)
 \end{aligned}$$

where d^n is the total distance of the ray path followed by the n -reflection, d_i the different stretches in which d^n can be divided (Figure 1) and u_i, v_i the parametrical coordinates that define the surface i (see references [12-14]). As can be seen, it is necessary to minimize a function of $2n$ variables. The problem is that the cost of this minimization increases exponentially with n .

The objective of the method proposed in this paper is to analyze electrically large bodies with multiple reflections and diffractions between its parts by computing efficiently the PO integrals using the SPM without the cumbersome and time-consuming problems of minimizing a function of n variables as demand the inverse ray tracing methods or the need to shooting a huge number of ray tubes as requires the SBR method. The proposed method combines the interpolation of the induced current by means of the current modes proposed in [15] with the SPM [16, 17] to obtain the scattered field. As stated in [15] the current is interpolated by means of a Bezier surface from the induced currents on a set of sampling points over the surface. Given the behavior of Bezier surfaces 8×8 sampling points are a number optimum for a good representation of the current. After the interpolation the critical points of SPM can be obtained minimizing the phase function of the PO integrand that includes the phase of the induced current. As it will be described below, there is no relationship between the SPM critical points and the control points. Therefore, the interpolation process is independent of the SPM computation.

From that, an iterative method to compute multiple order reflections and/or diffractions has been developed. The method consists, basically, of calculating iteratively the induced current in each surface involved in the reflection to obtain the scattered field at the reflection point. In each surface the induced current is expressed in terms of a current

mode. The definition of a current mode is an exponential function whose amplitude and phase are smooth functions that can be easily interpolated from their values in a reduced number of sampling points. The current in the sampling points in a surface (passive surface) is obtained from the fields at that points due the current mode defined in a surface (active surface) that is illuminating by reflection the passive surface. These fields are computed by the SPM and as it will be shown. To perform this computation it is only necessary the minimization of several functions of two variables, avoiding the minimization of functions of more than two variables necessary in the inverse methods and the shooting of a large amount of rays necessary in the SBR, reducing consequently the computation time as will be illustrated in the Results section. Once the current mode in the passive surface has been obtained, this surface is considered as the active surface and therefore it will illuminate a new surface (the new passive surface) in the next step of an iterative procedure to solve the multiple iteration problems arising in scattering and radiation problems with complex bodies.

The proposed method is advantageous with respect to the SBR because it provides the possibility of the computation of multiple interactions between large objects sampling the surface of the objects with a low amount of points, amount which is independent of the frequency. On the other hand with respect to the inverse methods presented in [10-12], the advantage is that the functions to minimize depends only on two variables, independently of the number of surfaces involved in the multiple interaction. These advantages are possible due to the most important technical combination of this paper: the combination of the SPM with the interpolation of the induced currents over a body by using Bézier surfaces.

It is important to bring out that the presented approach can be considered iterative in the sense that the PO current integrated by the SPM in the surface for a multiple interaction is computed iteratively for a surface taking into account the current of the surface considered in the previous iteration using in each surface the classical PO approach. There are other Iterative Physical Optics (IPO) approaches in the literature, which basically try to solve the Magnetic Field Integral Equation (MFIE) using IPO [18, 19] as an alternative of a matrix solution of the MFIE. The idea of our approach is not to solve any integral equation, but to provide an alternative to the classical ray methods used to compute higher order contributions in high frequency.

This paper is arranged as follows. Part 2 summarizes the procedure to obtain by interpolation the phase and amplitude functions that define a current mode. Part 3 shows how to compute the PO

integral due to a current mode for an observation point in the near or the far field by using the SPM. The iterative method considered for the computation of the multiple interactions between the different surfaces of a complex body is described in Part 4. Results for problems with double reflection, triple reflection and higher order reflection in a rectangular cavity are presented in Part 5 to show the performances of the proposed approach. Finally, in Part 6, the conclusions and the main features of the approach are summarized.

II. INTERPOLATION OF THE INDUCED CURRENT BY BÉZIER SURFACES

As mentioned above, the interpolation of the induced current was outlined in [15] and consists basically in using, as parameter interpolating function for each current mode, a Bézier surface to interpolate each component of the amplitude vector and another to interpolate the phase function. To interpolate the bi-dimensional scalar function Φ from a set of $(m+1)(n+1)$ values of the function, the control points of the Bézier surface are obtained by solving the following equation:

$$\mathbf{b} = \mathbf{U}^{-1} \Phi \mathbf{V}^{-1} \quad (2)$$

where:

$$\mathbf{b} = \begin{bmatrix} \bar{b}_{00} & \cdots & \bar{b}_{0n} \\ \vdots & \ddots & \vdots \\ \bar{b}_{m0} & \cdots & \bar{b}_{mn} \end{bmatrix}_{(m+1)(n+1)} \quad (3)$$

$$\Phi = \begin{bmatrix} \bar{\varphi}_{00} & \cdots & \bar{\varphi}_{0n} \\ \vdots & \ddots & \vdots \\ \bar{\varphi}_{m0} & \cdots & \bar{\varphi}_{mn} \end{bmatrix}_{(m+1)(n+1)} \quad (4)$$

$$\mathbf{U} = \begin{bmatrix} B_0(u_0) & \cdots & B_m(u_0) \\ \vdots & \ddots & \vdots \\ B_0(u_m) & \cdots & B_m(u_m) \end{bmatrix}_{(m+1)(m+1)} \quad (5)$$

$$\mathbf{V} = \begin{bmatrix} B_0(v_0) & \cdots & B_n(v_0) \\ \vdots & \ddots & \vdots \\ B_0(v_n) & \cdots & B_n(v_n) \end{bmatrix}_{(n+1)(n+1)} \quad (6)$$

\bar{b}_{ij} being the control points which define the surface which interpolates the function Φ , $\bar{\varphi}_{ij}$ the sampling points of that function, and B_i the Bernstein polynomials in terms of which the Bézier surface is expressed [13,14].

The interpolation can be performed taking 8×8 samples over the surface for a good representation of the current, taking into account the behavior of Bezier

surfaces as described in [13]. The samples are usually chosen equally spaced, although it is not a mandatory condition.

III. CALCULATION OF A SIMPLE REFLECTION USING THE STATIONARY PHASE METHOD AND CURRENT MODES

The use of the SPM to obtain the radiated field of an antenna in presence of a convex object and calculate the PO integral was shown in [12]. SPM is a mathematical approach that is especially suitable to calculate integrals with rapid oscillation of the integrand phase. This situation is given for the PO integral in high frequency. For this reason, SPM is advantageous for high frequency electromagnetic analysis with respect to classical numerical techniques such as the Gauss quadratures. The SPM requires the search of a set of critical points: stationary phase or internal points, boundary points and vertex points which give the first, second and third order contribution to the PO integral. In this section, we will concentrate on the application of the current modes to obtain the first order contribution, i.e., the contribution made by the stationary phase points, to the PO integral. The other contributions could be obtained in a similar way.

Consider a body in which the electric and magnetic currents have been defined in terms of current modes. The scattered field at an observation point $\bar{\mathbf{r}}$ can be obtained by computing the PO integral on the surface S' of that object:

$$\begin{aligned} \bar{\mathbf{E}}^S(\bar{\mathbf{r}}) &= \bar{\mathbf{E}}_J^S(\bar{\mathbf{r}}) + \bar{\mathbf{E}}_M^S(\bar{\mathbf{r}}) = \\ &= -j\lambda^{-1} \left(\int_{S'} (\hat{\mathbf{k}}_s \times \bar{\mathbf{J}}(\bar{\mathbf{r}}') \times \hat{\mathbf{k}}_s) \frac{e^{jk_s(\bar{\mathbf{r}}-\bar{\mathbf{r}}')}}{|\bar{\mathbf{r}}-\bar{\mathbf{r}}'|} dS \right) + \\ &+ j\eta\lambda^{-1} \left(\int_{S'} (\hat{\mathbf{k}}_s \times \bar{\mathbf{M}}(\bar{\mathbf{r}}')) \frac{e^{jk_s(\bar{\mathbf{r}}-\bar{\mathbf{r}}')}}{|\bar{\mathbf{r}}-\bar{\mathbf{r}}'|} dS \right) \end{aligned} \quad (7)$$

where $\bar{\mathbf{E}}_J^S(\bar{\mathbf{r}})$ and $\bar{\mathbf{E}}_M^S(\bar{\mathbf{r}})$ are the contributions of the induced electric and magnetic current mode $\bar{\mathbf{J}}(\bar{\mathbf{r}}')$ and $\bar{\mathbf{M}}(\bar{\mathbf{r}}')$ to the radiated field, λ is the wavelength, η is the impedance in free space and $\hat{\mathbf{k}}_s$ is the direction of observation for far field or the unit vector which joins the point $\bar{\mathbf{r}}'$ over the surface with the observation point for near field $\left(\frac{\bar{\mathbf{r}}-\bar{\mathbf{r}}'}{|\bar{\mathbf{r}}-\bar{\mathbf{r}}'|} \right)$. The induced currents can be expressed as follows:

$$\vec{J}(\vec{r}') = \hat{n} \times \begin{bmatrix} 1 - \Gamma_s & 0 \\ 0 & 1 - \Gamma_h \end{bmatrix} \begin{bmatrix} H_s^i(\vec{r}') \\ H_h^i(\vec{r}') \end{bmatrix} \quad (8)$$

$$\vec{M}(\vec{r}') = -\hat{n} \times \begin{bmatrix} 1 + \Gamma_s & 0 \\ 0 & 1 + \Gamma_h \end{bmatrix} \begin{bmatrix} E_s^i(\vec{r}') \\ E_h^i(\vec{r}') \end{bmatrix} \quad (9)$$

where \hat{n} is the unit vector normal to the surface at point \vec{r}' , Γ_s , and Γ_h are the Fresnel reflection coefficients [4], and $H_{s,h}^i$ and $E_{s,h}^i$ are the soft and hard components (perpendicular and parallel components respectively, see [4]) of the incident magnetic and electric fields at that point of the surface.

The two terms $\vec{E}_J^S(\vec{r})$ and $\vec{E}_M^S(\vec{r})$ of equation (7) can be written as follows, expressing the current by means of the amplitude and phase terms:

$$\vec{E}_J^S(\vec{r}) = -j\lambda^{-1} \left(\int_{S'} (\hat{k}_s \times \vec{J}_0(\vec{r}') \times \hat{k}_s) \frac{e^{jk[\hat{k}_s(\vec{r}-\vec{r}')+\phi(r')]}{|\vec{r}-\vec{r}'|} dS \right) \quad (10)$$

$$\vec{E}_M^S(\vec{r}) = j\eta\lambda^{-1} \int_{S'} (\hat{k}_s \times \vec{M}_0(\vec{r}')) \frac{e^{jk[\hat{k}_s(\vec{r}-\vec{r}')+\phi(r')]}{|\vec{r}-\vec{r}'|} dS \quad (11)$$

where $\vec{J}_0(\vec{r}')$, $\vec{M}_0(\vec{r}')$ are the amplitude values of the electric and magnetic current respectively at a point \vec{r}' on the surface, and $\phi(\vec{r}')$ is the phase. These functions define the corresponding current mode and it is assumed they are approximated by the Bézier surface described in part 2.

To apply the SPM, the amplitude functions can be expressed as:

$$g_J(\vec{r}') = \frac{\hat{k}_s \times \vec{J}_0(\vec{r}') \times \hat{k}_s}{|\vec{r}-\vec{r}'|} \quad (12)$$

$$g_M(\vec{r}') = \frac{\hat{k}_s \times \vec{M}_0(\vec{r}')}{|\vec{r}-\vec{r}'|} \quad (13)$$

and the phase function is expressed as:

$$f(\vec{r}') = \hat{k}_s |\vec{r}-\vec{r}'| + \phi(\vec{r}') = \begin{cases} \hat{k}_s \cdot \vec{r}' & \text{for observation in far field} \\ |\vec{r}-\vec{r}'| & \text{for observation in near field.} \end{cases} \quad (14)$$

Two integrals must be solved, one for the electric current and the other for the magnetic current. In parametric coordinates we have:

$$I_J = \int_{u=0}^{u=1} \int_{v=0}^{v=1} g_J(u, v) e^{jkf(u, v)} du dv \quad (15)$$

$$I_M = \int_{u=0}^{u=1} \int_{v=0}^{v=1} g_M(u, v) e^{jkf(u, v)} du dv. \quad (16)$$

Both integrals satisfy the conditions for the application of the SPM method [16,17]. The first step in solving the integrals is to find the critical points. As mentioned above, only the internal points will be considered here. These are the points with the parametric coordinates (u_s, v_s) , where function $f(u, v)$ has a minimum, i.e., where the parametric derivatives at this point are zero:

$$\begin{cases} f_u(u_s, v_s) = \frac{\partial f}{\partial u}(u_s, v_s) = 0 \\ f_v(u_s, v_s) = \frac{\partial f}{\partial v}(u_s, v_s) = 0. \end{cases} \quad (17)$$

The derivatives of the function $f(u, v)$ are:

$$f_u(u, v) = \begin{cases} \frac{\partial \hat{k}_s \cdot \vec{r}'}{u} + \frac{\partial \phi(\vec{r}')}{u} & \text{far field observation} \\ \frac{\partial |\vec{r}-\vec{r}'|}{u} + \frac{\partial \phi(\vec{r}')}{u} & \text{near field observation} \end{cases} \quad (18)$$

$$f_v(u, v) = \begin{cases} \frac{\partial \hat{k}_s \cdot \vec{r}'}{v} + \frac{\partial \phi(\vec{r}')}{v} & \text{far field observation} \\ \frac{\partial |\vec{r}-\vec{r}'|}{v} + \frac{\partial \phi(\vec{r}')}{v} & \text{near field observation} \end{cases} \quad (19)$$

where

$$\begin{aligned} \frac{\partial |\vec{r}-\vec{r}'|}{\partial u} &= \frac{-2(x-x')^2 \frac{\partial x'}{\partial u} - 2(y-y')^2 \frac{\partial y'}{\partial u} - 2(z-z')^2 \frac{\partial z'}{\partial u}}{2\sqrt{(x-x')^2 + (y-y')^2 + (z-z')^2}} \\ &= -\hat{k}_s \cdot \frac{\partial \vec{r}'}{\partial u} \end{aligned} \quad (20)$$

$$\begin{aligned} \frac{\partial |\vec{r}-\vec{r}'|}{\partial v} &= \frac{-2(x-x')^2 \frac{\partial x'}{\partial v} - 2(y-y')^2 \frac{\partial y'}{\partial v} - 2(z-z')^2 \frac{\partial z'}{\partial v}}{2\sqrt{(x-x')^2 + (y-y')^2 + (z-z')^2}} \\ &= -\hat{k}_s \cdot \frac{\partial \vec{r}'}{\partial v} \end{aligned} \quad (21)$$

$$\frac{\partial \hat{\mathbf{k}}_s \cdot \bar{\mathbf{r}}'}{\partial \mathbf{u}} = \hat{\mathbf{k}}_s \cdot \frac{\partial \bar{\mathbf{r}}'}{\partial \mathbf{u}} \quad (22)$$

$$\frac{\partial \hat{\mathbf{k}}_s \cdot \bar{\mathbf{r}}'}{\partial \mathbf{v}} = \hat{\mathbf{k}}_s \cdot \frac{\partial \bar{\mathbf{r}}'}{\partial \mathbf{v}} \quad (23)$$

$\frac{\partial \phi(\bar{\mathbf{r}}')}{\mathbf{u}}$ and $\frac{\partial \phi(\bar{\mathbf{r}}')}{\mathbf{v}}$ can be easily obtained as the

derivatives of the current mode and $\frac{\partial \bar{\mathbf{r}}'}{\mathbf{u}}$ and $\frac{\partial \bar{\mathbf{r}}'}{\mathbf{v}}$ can be obtained as the derivatives of the Bézier surface which describes the scattered object. The expressions for the derivatives of a Bézier surfaces can be seen in reference [13].

Then, if the derivatives of the Bézier surface which describes the body are denoted as $\bar{\mathbf{r}}'_u$ and $\bar{\mathbf{r}}'_v$, the system of equations to solve is the following, corresponding the sign + to observation in far field and the sign - to observation in near field:

$$\begin{cases} \left(\frac{\partial \phi(\bar{\mathbf{r}}')}{\mathbf{u}} \right) \pm \hat{\mathbf{k}}_s \cdot \bar{\mathbf{r}}'_u \Big|_{(u_s, v_s)} = 0 \\ \left(\frac{\partial \phi(\bar{\mathbf{r}}')}{\mathbf{v}} \right) \pm \hat{\mathbf{k}}_s \cdot \bar{\mathbf{r}}'_v \Big|_{(u_s, v_s)} = 0. \end{cases} \quad (24)$$

The Conjugate Gradient Method [20] has been used to solve the system of equations in our examples. Once the critical point has been obtained, its contribution to the PO integral is expressed as follows [12]:

$$\begin{aligned} \bar{I}_J &= \frac{\pi}{k} \frac{e^{jk[\hat{\mathbf{k}}_s(\bar{\mathbf{r}} - \bar{\mathbf{r}}'(u_s, v_s)) + \phi(u_s, v_s)]}}{|\bar{\mathbf{r}} - \bar{\mathbf{r}}'(u_s, v_s)|} \\ &\times \frac{\hat{\mathbf{k}}_s \times \bar{J}_0(u_s, v_s) \times \hat{\mathbf{k}}_s}{\sqrt{|f_{uu}^S \cdot f_{vv}^S - (f_{uv}^S)^2|}} e^{j\frac{\pi}{4}\sigma(\delta+1)} \end{aligned} \quad (25)$$

$$\begin{aligned} \bar{I}_M &= \frac{\pi}{k} \frac{e^{jk[\hat{\mathbf{k}}_s(\bar{\mathbf{r}} - \bar{\mathbf{r}}'(u_s, v_s)) + \phi(u_s, v_s)]}}{|\bar{\mathbf{r}} - \bar{\mathbf{r}}'(u_s, v_s)|} \\ &\times \frac{\hat{\mathbf{k}}_s \times \bar{M}_0(u_s, v_s)}{\sqrt{|f_{uu}^S \cdot f_{vv}^S - (f_{uv}^S)^2|}} e^{j\frac{\pi}{4}\sigma(\delta+1)} \end{aligned} \quad (26)$$

with

$$\sigma = \text{sign}(f_{uv}^S) \quad \text{and} \quad \delta = \text{sign}\left[f_{uu}^S \cdot f_{vv}^S - (f_{uv}^S)^2\right],$$

f_{uu}^S , f_{vv}^S and f_{uv}^S being the second derivatives of the phase at the point (u_s, v_s) . These are easily computed, deriving (18) and (19):

$$\begin{aligned} f_{uu}^S &= \frac{\partial}{\mathbf{u}} \left(\frac{\partial \phi(\bar{\mathbf{r}}')}{\mathbf{u}} \pm \hat{\mathbf{k}}_s \cdot \bar{\mathbf{r}}'_u \right) \Big|_{(u_s, v_s)} \\ &= \frac{\partial^2 \phi(\bar{\mathbf{r}}')}{\mathbf{u}^2} \pm \hat{\mathbf{k}}_s \cdot \bar{\mathbf{r}}''_{uu} \pm \frac{1}{|\hat{\mathbf{k}}_s|} \times \\ &\quad \left\{ (\bar{\mathbf{r}}'_u \cdot \bar{\mathbf{r}}'_u) - (\bar{\mathbf{r}}'_u \cdot \hat{\mathbf{k}}_s)^2 \right\} \Big|_{(u_s, v_s)} \end{aligned} \quad (27)$$

$$\begin{aligned} f_{vv}^S &= \frac{\partial}{\mathbf{v}} \left(\frac{\partial \phi(\bar{\mathbf{r}}')}{\mathbf{v}} \pm \hat{\mathbf{k}}_s \cdot \bar{\mathbf{r}}'_v \right) \Big|_{(u_s, v_s)} \\ &= \frac{\partial^2 \phi(\bar{\mathbf{r}}')}{\mathbf{v}^2} \pm \hat{\mathbf{k}}_s \cdot \bar{\mathbf{r}}''_{vv} \pm \frac{1}{|\hat{\mathbf{k}}_s|} \times \\ &\quad \left\{ (\bar{\mathbf{r}}'_v \cdot \bar{\mathbf{r}}'_v) - (\bar{\mathbf{r}}'_v \cdot \hat{\mathbf{k}}_s)^2 \right\} \Big|_{(u_s, v_s)} \end{aligned} \quad (28)$$

$$\begin{aligned} f_{uv}^S &= \frac{\partial}{\mathbf{u}} \left(\frac{\partial \phi(\bar{\mathbf{r}}')}{\mathbf{v}} \pm \hat{\mathbf{k}}_s \cdot \bar{\mathbf{r}}'_v \right) \Big|_{(u_s, v_s)} \\ &= \frac{\partial^2 \phi(\bar{\mathbf{r}}')}{\mathbf{u}\mathbf{v}} \pm \hat{\mathbf{k}}_s \cdot \bar{\mathbf{r}}''_{uv} \pm \frac{1}{|\hat{\mathbf{k}}_s|} \times \\ &\quad \left\{ (\bar{\mathbf{r}}'_u \cdot \bar{\mathbf{r}}'_v) - (\bar{\mathbf{r}}'_u \cdot \hat{\mathbf{k}}_s)(\bar{\mathbf{r}}'_v \cdot \hat{\mathbf{k}}_s) \right\} \Big|_{(u_s, v_s)} \end{aligned} \quad (29)$$

In equations (27-29) the sign + corresponds to observation in far field and the sign - to observation in near field. It is important to take into account the possibility of not all the surface is illuminated. In this case, only the illuminated part of the surface is considered to interpolate the current. Then, it appears a shadow boundary which contribution should be considered introducing a second order critical point as is shown in [12].

Equations (25) and (26) illustrate the advantage of the SPM with respect to other numerical integration techniques, because the value of the integral is reduced to the evaluation of a closed formula to evaluate the contribution of each critical point and the further summation of all the contributions. As it is stated in [12], there is, as much, only one first order critical point, four second order critical points and four third order critical points in each parametric surface that defines the geometry. On the other hand, there is necessary to evaluate the integrand for a high amount of points in a classical numerical integration technique (usually with an step of $\lambda/10$ in the PO application, due to the rapid variation of the integrand's phase). Therefore, the number of operations involved in the calculation of the integral using the SPM is clearly inferior giving the computational advantage of this technique for integrals with rapidly variation integrand's phase,

typical situation in the analysis of electrically large electromagnetic problems.

It is also important to highlight that the position of the critical point is independent of the sampling points chosen to interpolate the current, being both procedures (the interpolation and the SPM computation) completely independent. In this section, the objective is only to show the applicability of the current interpolation to the analysis of scattered field by means by SPM, but there is not advantage with respect to the SPM computation without current interpolation. The advantage appears, as it is stated in next Section, when multiple interactions between different parts of a complex body must be considered to obtain the total scattered field.

An example is presented here to show the accuracy of the application of the current interpolation to the SPM. In the example, indicated in Figure 2, a comparison between the results obtained with the proposed approach and those obtained using a GTD/UTD is presented. The GTD/UTD results have been obtained with the code FASANT whose accuracy has been proven in [10]. The surface in Figure 2 is a quarter of a sphere whose sides are $2.35\lambda \times 2.35\lambda$. The frequency is 300 MHz. The surface is a perfect electric conductor coated with an absorbing material that has both electric and magnetic losses with $\epsilon_r=2.5-j1.25$, $\mu_r=1.6-j0.8$ and a thickness of $\tau=0.15\lambda$. The electromagnetic illumination is by a vertical dipole placed at 12λ from the center of the sphere. The dipole's coordinates are $(2.0,3.0,0.0)$ and it is orientated according to the Z-axis of the reference system (X, Y, Z) depicted in Figure 2. The observation points are located along a line from $(4.0,2.0,0.0)$ to $(4.0,2.0,4.0)$. The minimum distance from the surface is 14.9λ . The comparison of the results of both methods is depicted in Figure 3, in which a close correspondence between both results can be observed.

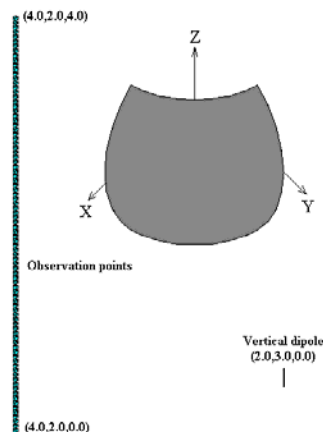


Fig. 2. Spherical section illuminated by a dipole. Position of the observation points where the scattered field is computed.

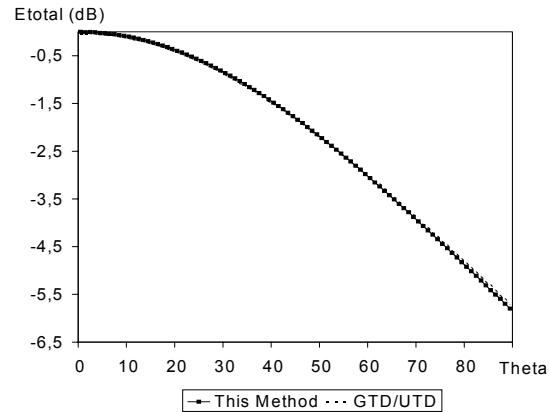


Fig. 3. Scattered field by the spherical sector illuminated by a vertical dipole.

IV. ITERATIVE METHOD FOR THE COMPUTATION OF HIGHER ORDER REFLECTIONS

When only single reflections are to be evaluated, the usage of the current interpolation approach, presented in Section 3 is not advantageous, because it replaces the minimization of the function distance that, in this case, depends on two variables, by the minimization of an interpolated phase function that depends also on two variables. Therefore, there is no gain in the minimization procedure. Moreover, the interpolation of the phase function requires the prior evaluation of the current at a set of sampling points and the corresponding interpolation using parametric interpolating surfaces. Therefore, the computation time is higher than when using a direct ray tracing to compute the stationary phase points, as stated in [12]. However, the application of a direct ray-tracing to obtain multiple reflections is much more complex, because it requires the minimization of a function with $2n$ variables, which exponentially increases the computation with n , as was mentioned in the introduction.

The solution proposed in this paper consists of applying an iterative method in which the current induced over the surfaces involved in the multiple reflections is computed sequentially. Therefore, to obtain the current induced over a surface, it is necessary to know the current over the previous one. The interpolation method is used, as it only needs to store a small amount of information to accomplish this calculation.

Let us suppose a surface that we will call active surface, over which its induced current is defined by means of the current value at a set of control points. We will compute the induced current over another

surface (the passive surface), induced by the field radiated by the currents of the active surface. For that, a mesh of points over the passive surface is defined as depicted in Figure 4. In this mesh, we will compute the impressed field and from that the corresponding induced current. The mesh corresponds to the control points, which interpolate the current surface and the impressed field at each control point of the passive surface can be computed using the interpolated current of the active surface following the procedure described in Section 3.

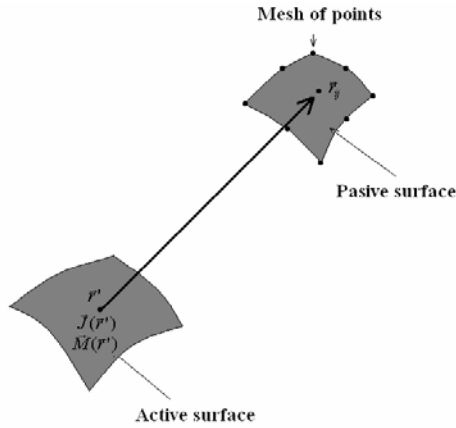


Fig. 4. Interpolation of the current on the passive surface.

This procedure can be applied iteratively. Beginning at the source that illuminates a certain structure, the radiated field can be obtained in a given direction from the multiple reflections produced. The iterative method is carried out as follows:

- a) The surfaces illuminated by the source are determined. These are the passive surfaces in the first iteration.
- b) The impressed field at a set of sampling points is computed for each passive surface. From these values the equivalent currents are interpolated.
- c) The next iteration starts. The passive surfaces become active.
- d) The surfaces illuminated by the active surfaces are determined. These become the passive surfaces.
- e) If it is the last iteration, it is checked. If not, the procedure is repeated from stage b.

An important task in the procedure is to select the passive surfaces for a given active surface. If there is not prior knowledge of which these surfaces are, all the surfaces of the model can be passive except the active. However, as it is stated in [21] the stationary phase points of the SPM correspond to the reflection points of Geometrical Optics. Therefore, the ray that joins the source with the stationary phase point and

the one that joins this point with the observation point must satisfy the Snell's law. From that, a previous selection of passive surfaces can be accomplished, determining the region of the space that satisfies the Snell's law from any point of the active surface. Only the surfaces places total or partially inside of this region can be passive surfaces. This previous selection allows reducing considerably the number of passive surfaces selected and, as a consequence, the time required for the iterative procedure. A similar reasoning can be done for the boundary and vertex critical points according of the properties of such points, described in [21].

An example with three surfaces illuminated by a plane wave with a direction of incidence \hat{k}_i , is depicted in Figure 5. Surface 1 is selected as the passive surface for the first step of the scheme, calculating the impressed field at each control point of the surface and from this the equivalent currents, which are denominated $\vec{J}^{(1)}, \vec{M}^{(1)}$. Once these currents have been determined, surface 1 becomes the active surface.

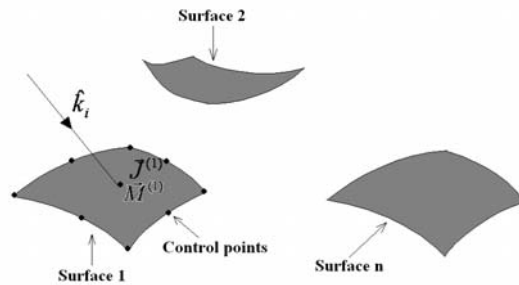


Fig. 5. First step of the iterative process. Computation of the induced currents by the incident plane wave.

The next step is to determine the radiation directions of the currents $\vec{J}^{(1)}, \vec{M}^{(1)}$ and to obtain the new passive surface. Surface 2 is the passive surface in our example. The impressed field over the control points of this surface is computed and the equivalent currents $\vec{J}^{(2)}, \vec{M}^{(2)}$ are obtained (Figure 6).

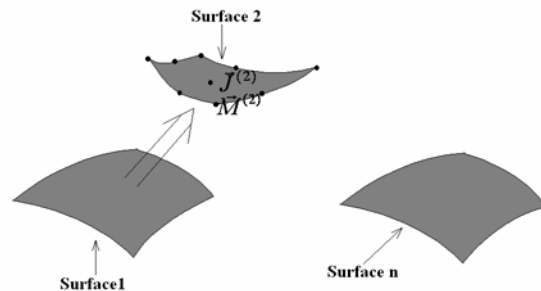


Fig. 6. Computation of the equivalent currents over surface 2 in the second step of the iterative process.

In the next step, surface 2 becomes the active surface and surface 3 the passive. The same procedure described above is applied and the equivalent currents on the surface 3 ($\vec{J}^{(3)}$, $\vec{M}^{(3)}$) are obtained. From these currents, the radiated field can be obtained (Figure 7).

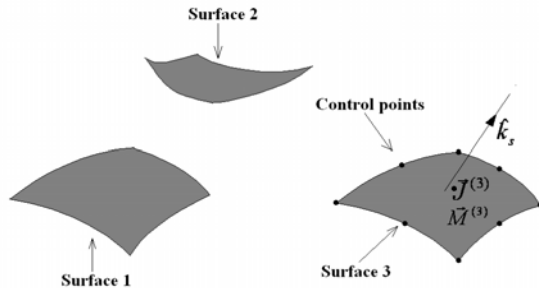


Fig. 7. Scattered field in the direction \hat{k}_s from the current calculated in the last step of the iterative process.

It is important to remark that to obtain the induced currents over the passive surfaces in each iteration, it is only necessary to calculate the radiated field by the previous surface (the active surface) from its induced currents. As these currents are represented by means of interpolated functions which depend only on the parametric coordinates of the active surface, each iteration requires several minimizations of functions of two variables, so many as sampling points are considered. Then, the minimization of a function of n variables mentioned in the introduction is being replaced by an iterative procedure consisting in the minimization of functions of two variables. As the number of sampling points in each surface is not necessary to be big as was proved in [15] the number of this functions to minimize is small and the computation time is reduced drastically as will be shown in the Results section.

V. RESULTS

In this section, the proposed method is validated comparing with the results obtained by the SPM without interpolation and by GTD/UTD for some simple cases. The comparison between the features both techniques (SPM and GTD/UTD) can be seen in [20]. These cases also illustrate the reduction in CPU time achieved with this method. After that, the application of the interpolation to a practical case is shown. The application considered is the computation of the RCS of a cavity. In this case, the proposed method is compared with the SBR, obtaining a considerable reduction in the CPU-time as it will be seen below.

The first case analyzed consists of the two surfaces indicated in Figure 8: one flat and other curved, with a curvature such that the normal vector at the surface turns at a maximum angle of 26° when it moves along the surface. We will call this angle the “maximum turning angle” of the surface. Both surfaces in Figure 8 have sides of 4 m, which is equivalent to 13.33λ and they are considered to be perfect electric conductors (PEC) coated with a material with electric and magnetic losses, characterized by a dielectric constant of $\epsilon_r=2.5-j1.25$, a magnetic constant of $\mu_r=1.6-j0.8$ and a thickness of 0.15λ . The geometry is illuminated by a vertical dipole placed at point $(0.0,-6.0,0.0)$ as shown in Figure 8. The observation points were situated along a line from $(0.0,0.0,6.0)$ to $(0.0,4.0,4.0)$. Figure 9 shows a clear agreement between results obtained with the proposed method and those obtained with GTD/UTD.

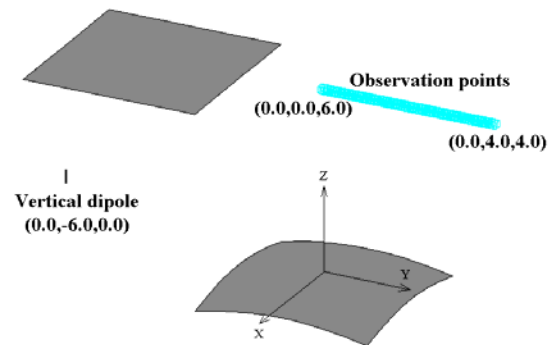


Fig. 8. Planar surface with 4 meters per side and convex surface with 4 meters per side and maximum turning angle of 26° .

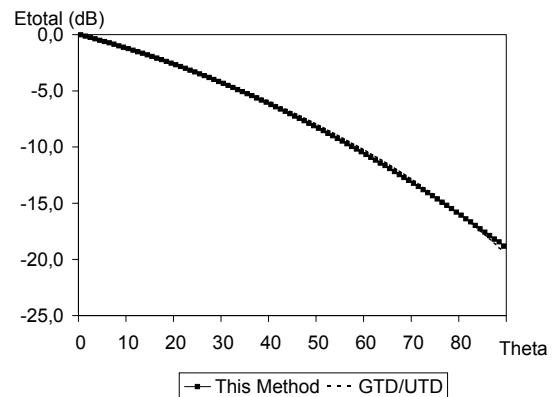


Fig. 9. Amplitude of the scattered field due to the double reflection between a planar surface and a convex surface coated with a material with losses.

The next geometry analyzed is depicted in Figure 10 and consists of three flat surfaces. The first is a PEC and the others are PECs coated with a material

with the same constants as the previous case. The plates have sides of 4 m (13.33λ). A vertical dipole was placed at $(0.0,6.0,0.0)$ and the radiated field is obtained after the third reflection along a line from $(0.0,-5.0,0.0)$ to $(0.0,-9.0)$ consisting of 90 points. The comparison between the predicted values using our approach and those obtained with GTD/UTD is presented in Figure 11.

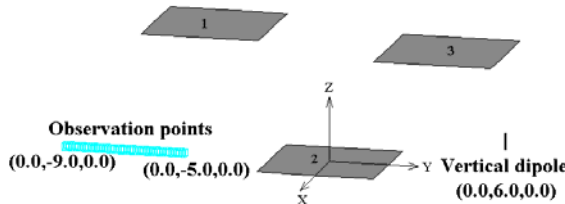


Fig. 10. Three planar surfaces.

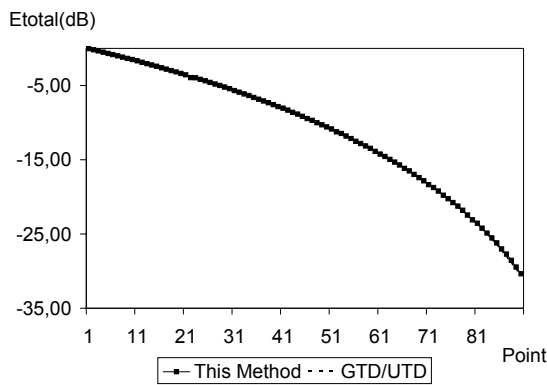


Fig. 11. Amplitude of the scattered field due to the triple reflection produced by three planar surfaces, the first a PEC and the others PECs coated with a material with losses.

To demonstrate the efficiency of the proposed approach, we can compare the difference in CPU-time needed to analyze both a flat and a convex surface. Traditional SPM takes 33 seconds whilst the interpolation method takes just 5 seconds. Both results were obtained on a Pentium III with 1 GB of RAM. Taking into account that the CPU time for the field computation is practically the same, the difference is due to the advantage of the current interpolation. Traditional SPM has to minimize a function of four variables for each observation point (90 points in the example) in order to find the stationary phase points corresponding to each observation point. On the other hand, the interpolation method has to minimize a function of two variables to obtain the induced current in each sampling point of the second surface (64 points were used, 8 in each parametric direction) and another function of two variables to find the stationary phase point corresponding to each observation point. As the induced current only has to be computed once,

90 minimizations of a function of four variables are being replaced by 154 minimizations of functions of two variables. This fact allows for the time reduction mentioned above. Therefore, the method is efficient due to the reduction of the order of minimization.

Similar conclusions can be obtained with three flat surfaces where we replace 90 six-variables sets of minimizations by 218 two-variables sets of minimizations (64 for the induced current in the second surface, 64 for the induced current in the third surface and 90 to obtain the stationary phase point corresponding to each observation point). In this case, the GTD/UTD code FASANT used for the validation is unable to treat triple-reflections on curved surfaces, requires 15 minutes and 2 seconds to perform the analysis, while the interpolation method only needs 1 minute and 23 seconds.

Finally, as mentioned above, the result of the application of the proposed method to the analysis of the RCS of a cavity is shown. The case consists in a rectangular cavity whose dimensions are $30\lambda \times 10\lambda \times 10\lambda$ (see Figure 12). The monostatic RCS was obtained varying the incidence angle for directions contained in a symmetry plane of the cavity, which contain the axis of the aperture. Figure 13 illustrates the comparison of the interpolation method with the SBR for the theta polarization. As can be seen there is a good agreement between both results. However, the SBR takes 12 hours, 12 minutes and 18 seconds, considering 10.000 ray tubes launched from the aperture (with a separation between points of a tenth of wavelength, that is to say, 100 points per square wavelength), while the interpolation method only requires 58 minutes and 47 seconds, because only 64 points are considered in the interpolation. It is important to notice that in this case the authors only try to prove that the computational cost is importantly reduced with the proposed method with respect to the SBR to obtain the same results. Logically, the diffraction should be included in both approaches to improve the results. The diffraction could be easily introduced in our approach considering the contribution of the second and third order critical points in the SPM formulation. The procedure would be identical to the one described in Section 2.

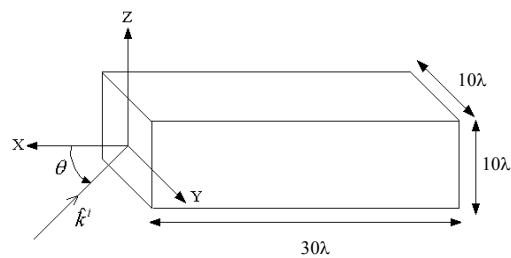


Fig. 12. Geometry of the rectangular cavity analyzed.

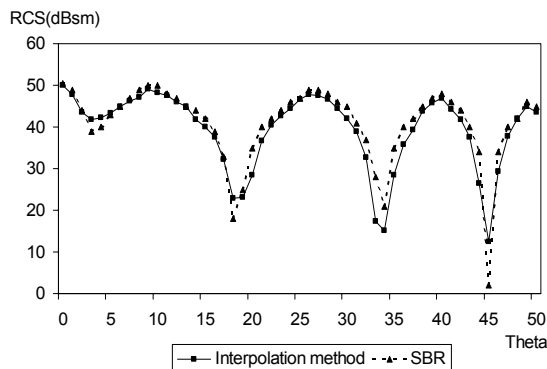


Fig. 13. Comparison between the results obtained by the interpolation method and the SBR for the monostatic RCS of the rectangular cavity.

VI. CONCLUSIONS

A method for obtaining higher order contributions to the electromagnetic scattered field by complex bodies has been developed. The method is based on the interpolation of the induced currents, by means of Bézier surfaces. For each current mode, it uses one Bézier surface to interpolate each component of the amplitude and another one to interpolate the phase. Once it has interpolated these induced currents, the scattered field is obtained by solving the PO integral using the SPM.

The method has several advantages over others currently being used to obtain these higher order contributions. The method can be used with all surfaces not only flat ones like the Image Method. The number of sampling points required to interpolate the current on a surface is very low compared to the number of rays the SBR uses to solve these kinds of problems. Finally, the advantage the proposed approach over ray-tracing inverse methods is that it only needs to minimize functions of two variables to find the ray-path, irrespectively of the order of the contribution. Whilst inverse methods need minimize functions of $2n$ variables, n being the order of the contribution, which means that the CPU-time needed for each minimization, increases exponentially with n .

The method developed is especially suitable for the analysis of problems where higher order contributions are of importance such as the propagation of tunnels or the computation of the RCS of cavities. An example of the last application has been shown in the Results section.

ACKNOWLEDGEMENTS

This work has been supported in part by Universidad de Alcalá, Project UAH PI2005/069.

REFERENCES

- [1] M.C.Lawton, and J.P.McGeehan, "The application of a deterministic ray launching algorithm for the prediction of radio channel characteristics in small-cell environments," *IEEE Transactions on Vehicular Technology*, vol 43, no. 4, November 1994, pp. 955-969.
- [2] S.Y.Tan, and H.S.Tan, "A microcellular communications propagation model based on the Uniform theory of Diffraction and Multiple Image Theory," *IEEE Transactions on Antennas and Propagation*, vol 44, No. 10, October 1996, pp. 1317-1326.
- [3] M. Domingo, R.P. Torres, and M.F. Cátedra, "Calculation of the RCS from the Interactions of Edges and Facets," *IEEE Transactions on Antennas and Propagation*, vol 42, no 6, June 1994, pp.885-890.
- [4] C.A. Balanis, *Advanced Engineering Electromagnetics*. John Wiley & Sons, New York, 1989.
- [5] H. Ling, R. Chou, and S.W. Lee, "Shooting and Bouncing Rays: Calculating the RCS of an Arbitrary Shaped Cavity," *IEEE Transactions on Antennas and Propagation*, vol. 37, February 1989, pp. 194-205.
- [6] S.W. Lee, H. Ling, and R. Chou, "Ray-Tube Integration in Shooting and Bouncing Ray Method," *Microwave & Optical Technology Letters*, vol. 1, no. 8, Aug. 1988, pp. 286-289.
- [7] S.K. Jeng, "Near-Field Scattering by Physical Theory of Diffraction and Shooting and Bouncing Rays," *IEEE Transactions on Antennas and Propagation*, vol. 46, no. 4, April 1998, pp. 551-558.
- [8] S.Y.Seidel, and T.S.Rappaport, "Site-Specific propagation prediction for wireless in building personal communication system design," *IEEE Transactions on Vehicular Technology*, vol. 43, no. 4, November 1994, pp.879-891.
- [9] H.T. Anastassiou, "A Review of Electromagnetic Scattering Analysis for Inlets, Cavities and Open Ducts," *IEEE Antennas and Propagation Magazine*, vol. 45, no 6, December 2003, pp. 27-40.
- [10] J. Pérez, F. Sáez de Adana, O. Gutiérrez, I. González, M.F. Cátedra, I. Montiel, and J. Guzmán, "FASANT: Fast Computer Tool for the Analysis of On-Board Antennas," *IEEE Antennas*

- and *Propagation Magazine*, vol. 41, no 2, April 1999, pp. 94-99.
- [11] M. F. Cátedra, J. Pérez, F. Sáez de Adana, and O. Gutiérrez, "Efficient ray-tracing techniques for 3D analysis of propagation in mobile communications. Application to picocell and microcell scenarios," *IEEE Antennas and Propagation Magazine*, vol. 40, no. 2, April 1998, pp. 15-28.
- [12] O.M. Conde, J. Pérez, and M. F. Cátedra, "Stationary Phase Method Application for the Analysis of Radiation of Complex 3-D Conducting Structures," *IEEE Transactions on Antennas & Propagation*, vol. 49, no. 5, pp. 724-731, May 2001.
- [13] G.E. Farin, *Curves and Surfaces for Computer Aided Geometric Design, A Practical Guide* 2nd edition, Academic Press Inc., London 1990.
- [14] C. de Boor, *A practical guide to splines*. Springer, Berlin, 1978.
- [15] O. Gutiérrez, F. Sáez de Adana, F. Rivas, I. González, and M. F. Cátedra, "Method to Interpolate Induced Currents with a Low Amount of Sample Points by Means of Bézier Surfaces," *Electronic Letters*, vol. 39, no. 2, pp. 177-178, January 2003.
- [16] D. S. Jones, and M. Kline, "Asymptotic Expansions of Multiple Integrals and the Method of the Stationary Phase," *Journal of Mathematical Physics*, Vol. 37, January 1957.
- [17] J. C. Cooke, "Stationary Phase in Two Dimensions," *IMA Journal of Applied Mathematics*, vol. 29, pp. 25-37, 1982.
- [18] F. Obelleiro-Basteiro, J.L. Rodriguez, and R.J. Burkholder, "An Iterative Physical Optics Approach for Analyzing the Electromagnetic Scattering by Large Open-Ended Cavities," *IEEE Transactions on Antennas and Propagation*, vol. 43, no. 4, April 1995, pp. 356-361.
- [19] K. Sarabandi, and D. Zahn, "Numerical Simulation of Scattering from Rough Surfaces Using an Iterative Physical Optics Approach," *IEEE Antennas and Propagation Society International Symposium, 1998*. 21-26 June 1998, volume 2, pp:1070 – 1073.
- [20] W.H. Press, B.P. Flannery, S.A. Teukolsky, and W.T. Vetterling, *Numerical Recipes*. Cambridge University Press, Cambridge (Gran Bretaña). 1987.
- [21] O.M. Conde, F. Saez de Adana, and M.F. Cátedra, "A Comparison Between Two High-Frequency Techniques Applied to the Analysis of On-Board Antennas," *Microwave & Optical Technology Letters*, Vol. 36, n° 5, pp. 415-417, March 2003.



Francisco Saez de Adana was born in Santander, Spain, in 1972. He received the BS, MS and PhD. degrees in Telecommunications Engineering from the University of Cantabria, Spain, in 1994, 1996 and 2000, respectively. Since 1998 he works at the University of Alcalá, first as assistant professor and since 2002 as professor. He has worked as faculty research at Arizona State University from March 2003 to August 2003.

He has participated in more than forty research projects with Spanish, European, American and Japanese companies and universities, related with analysis of on board antennas, radio propagation in mobile communication, RCS computation, etc. He has directed two Ph. D. Dissertations, has published thirteen papers in referred journals and more than 30 conference contributions at international symposia. His research interests are in areas of high-frequency methods in electromagnetic radiation and scattering, on-board antennas analysis, radio propagation on mobile communications and ray-tracing acceleration techniques.



Oscar Gutiérrez Blanco was born in Torrelavega, Spain, in 1970. He received the BS and MS degrees in Telecommunications Engineering from the University of Cantabria, Spain, in 1993 and 1996, respectively. From 1995 to 1998, he was with the Communications Engineering Department of the Cantabria as Research assistant. He received the Ph.D. degree in Telecommunication from the Alcalá university, Spain, in 2002. From 1998 to 2000, he was with the Signal Theory and communications Department of the Alcalá University, Madrid. In 2001, he is currently an assistant professor in the Computational Science Department in the Alcalá University, Madrid.

He has participated in more than 40 research projects, with Spanish and European companies, related with analysis of on board antennas, radio propagation in mobile communication, RCS computation, etc. His research interests are in high-frequency methods in electromagnetic radiation and scattering, and ray-tracing acceleration techniques.



Lorena Lozano was born in Madrid, Spain, in 1978. She received the BS and MS degrees in Telecommunications Engineering from the University of Alcalá in 2000 and 2002, respectively. She is currently pursuing the Ph.D. degree at the Computer Science Department, University of Alcalá, Spain.

She has been with the Signal Theory and Communications Department of the University of Alcalá since 1999 to 2004 and, since then, in the Computer Science Department of the University of Alcalá. From June 2004 to November 2004, she was with the Electrical Engineering Department of Arizona State University, as a research assistant. Her research interests are in areas of high-frequency methods in electromagnetic radiation and scattering, on-board antennas analysis, ray-tracing acceleration techniques, and RCS computation.



Manuel F. Catedra received his M.S. and Ph. D. degrees in Telecommunications Engineering from the Polytechnic University of Madrid (UPM) in 1977 and 1982 respectively. From 1976 to 1989 he was with the Radiocommunication and Signal Processing Department of the UPM. He has been Professor at the University of Cantabria from 1989 to 1998. He is currently Professor at the University of Alcalá, in Madrid, Spain.

He has worked on about 60 research projects solving problems of Electromagnetic Compatibility in Radio and Telecommunication Equipment, Antennas, Microwave Components and Radar Cross Section and Mobile Communications. He has developed and applied CAD tools for radio-equipment systems such as Navy-ships, aircraft, helicopters, satellites, the main contractors being Spanish or European Institutions such as EADS, ALCATEL, CNES, ALENIA, ESA, DASA, SAAB, INTA, BAZAN, INDRA, the Spanish Defence Department.

He has directed about 15 Ph D. dissertations, has published about 45 papers (IEEE, Electronic Letters, etc), two books, about 10 chapters in different books, has given short courses and has given around a hundred and thirty presentations in International Symposia.